Control of the South Atlantic Convergence Zone by extratropical thermal forcing

Stefanie Talento[1] · Marcelo Barreiro[1]

Abstract The response of the South Atlantic Convergence Zone (SACZ) to an extratropical thermal forcing is investigated in a series of simulations performed with an atmospheric general circulation model coupled to a slab ocean model. Three sets of experiments are performed, varying the extratropical forcing. In the first the forcing consists of warming of the Northern Hemisphere (NH) and cooling of the Southern Hemisphere, with zero global average. In the second and third experiments, the former forcing is divided into its northern and southern components to asses their relative roles in affecting the SACZ. In all the cases realistic surface boundary conditions are implemented. We found that during its peak in austral summer the SACZ weakens in response to the extratropical forcing and that such weakening is mostly due to the NH component of the forcing. We found that 75% of the SACZ signal in response to the forcing is linked to the generation of a secondary tropical convergence zone in the Atlantic Ocean around 20°N–30°N, which generates an anomalous Hadley circulation with subsidence over the SACZ. This mechanism appears to be dependent on the upper level changes and tropical ocean response, as it weakens significantly when the simulation is repeated not allowing the tropical sea surface temperatures to change in response to the forcing. The remaining 25% of the signal can be explained through the development of a Walker-type of circulation between western tropical Africa and the SACZ, being this mechanism dependent on the African land surface temperature reaction to the remote forcing.

Keywords SACZ · Extratropical forcing · Tropical sea surface temperatures · Slab ocean model

* Stefanie Talento
stalento@fisica.edu.uy

[1] Department of Atmospheric Sciencies, Institute of Physics, School of Sciences, Universidad de la República, 11400 Montevideo, Uruguay

1 Introduction

The capability of an extratropical thermal forcing to affect the tropical climate has been suggested in studies analysing paleoclimatic data (Wang et al. 2004), twentieth century observations (Folland et al. 1986) and numerical simulations (Chiang and Bitz 2005; Kang et al. 2008, 2009; Frierson and Hwang 2012; Cvijanovic and Chiang 2013; Talento and Barreiro 2015: hereafter TB2015). The Intertropical Convergence Zone (ITCZ) has been the most studied feature and the general picture emerging from these studies is that the ITCZ tends to shift toward the warmer hemisphere. However, there is evidence supporting the idea that other features of the tropical climate might be affected by such an extratropical influence. In particular, the South Atlantic Convergence Zone (SACZ) stands out as one of such possibly affected features.

The SACZ is a summertime elongated convective belt orientated diagonally (in the NW-SE direction) extending from the Amazon basin to southeastern Brazil and the South Atlantic Ocean (Kodama 1992, Carvalho et al. 2004). The location of the SACZ is related to the upper-level circulation over South America during austral summer. In this season an anticyclonic circulation develops over Bolivia -the Bolivian High- together with a cyclonic circulation downstream over the northeast coast of Brazil; the SACZ is located between these two features (Garreaud and Aceituno 2007). The SACZ presents variability in many timescales from intraseasonal to decadal (Vera et al. 2006) and the main mode of variability is a dipole-like structure, with centers of opposite sign over the SACZ and southeastern South America (SESA; e.g. Doyle and Barros 2002).

Kodama (1993) finds that two conditions are necessary for the development of sub-tropical convergence zones (including the SACZ). First, a subtropical jet in the subtropical latitudes (30°S–35°S) and, second, a low-level poleward flow in the western boundary of the surrounding sub-tropical high. The low-level flow, indispensable for moisture transport, is formed geostrophically between the subtropical high and a low pressure system developed by continental heating; this flow together with the upper level subtropical jet produces a favourable configuration for frontogenesis and convective instability. Figueroa et al. (1995) further elaborate on the mechanisms promoting the development of the SACZ and succeed in simulating it in its observed climatological position by combining the effects of diabatic heating over the Amazon and the steep Andean topography on the regional basic flow. Topography in central-east Brazil has also proven to be fundamental for anchoring the SACZ in its present climatological location, as numerical simulations indicate that a southward SACZ shift will follow in the absence of these mountains (Grimm et al. 2007). The control of the SACZ by remote tropical or extratropical influences has also been noted in the literature. Grimm and Silva Dias (1995) analyse the influence functions of a simplified barotropic model and find that anomalous convection over the South Pacific Convergence Zone may affect the convection over the SACZ by deepening of an upper-lever trough in SESA.

The notion that the SACZ might react to extratropical forcing is supported by both paleoclimatic data and numerical simulations.

Stríkis et al. (2015) present a multi-proxy paleoprecipitation reconstruction of areas affected by SACZ and ITCZ during Heinrich stadial 1 (HS1). Heinrich stadials occur as massive depositional episodes of ice-rafted debris in the north Atlantic Ocean, implying an abrupt cooling of the northern midlatitudes of this basin. The authors find that the HS1 footprint is characterized by a southward shift of the ITCZ as well as an intensification of the SACZ, being the response to the northern hemisphere forcing synchronous.

Meanwhile, Chiessi et al. (2009) analyse the possible impact of the Atlantic Multidecadal Oscillation (AMO) on the South American Monsoon System using 4500 years-long proxy records of the La Plata River discharge variability. They suggest that during periods of positive AMO (characterized by a widespread NH warming in the north Atlantic Ocean) a northward migration of the ITCZ and cooling of the western South Atlantic would lead to a decrease in the intensity of the South American Low Level Jet (SALLJ), producing a decrease in precipitation over La Plata Basin.

Junquas et al. (2012) analyze the summer precipitation variability over SESA and SACZ under a global warming scenario in the CMIP3 simulations. They find that the future summer (December –February: DJF) precipitation variability over SESA and SACZ has a strong projection on the changes of the above mentioned dipole-pattern activity (also in agreement with Talento and Barreiro 2012). Their results indicate that in a global warming scenario, in which the Northern Hemisphere (NH) is expected to warm faster than the Southern Hemisphere (SH), there is an increase in the frequency of the positive phase of the dipole leading to wetter conditions over SESA and dryer ones over SACZ.

The existence of an interhemispheric thermal gradient in which the NH is warmer than the SH has been already noted in twentieth century observations in Friedman et al. (2013). The interhemispheric temperature asymmetry (ITA) annual mean (NH minus SH) shows an abrupt descent in the late 1960s while a linear upward trend is noticed from the 1980s. Although for the twentieth century no significant signal has been found linking SACZ precipitation and the ITA, following Junquas et al. (2012) and Talento and Barreiro (2012), some signal is expected to arise during the twenty-first century when the ITA is projected to rise continuously.

In this study we further explore the mechanisms through which the SACZ may respond to an extratropical thermal forcing. To do so we conduct a series of simulations performed with an atmospheric general circulation model (AGCM) coupled to a slab ocean model, prescribing realistic surface boundary conditions. In our first series of simulations the imposed extratropical forcing consists of warming of the NH and cooling of the SH, with zero global average. In order to determine which component of the extratropical forcing most affects the SACZ we conduct two complimentary experiments in which the former forcing is divided into its northern and southern components, respectively. The relative role of the tropical Sea Surface Temperatures (SSTs) in the communication of the remote signal will be assessed in an experiment in which the slab ocean model will be turned off over the tropics. As will be shown, when the tropical SSTs are not allowed to change there is still some signal over the SACZ and Africa, fact that motivates the last experiment in which the role of the African land surface temperature (LST) is investigated, not allowing it to change in response to the remote forcing. This paper builds upon the ideas presented in TB2015 but focusing on the SACZ and, therefore, changing the focus to austral summer instead of annual means.

The manuscript is organized as follows: In Sect. 2 we introduce the model and the experiments. Results are presented in Sects. 3 and 4. In Sect. 3 we present the experiments where the slab ocean model is applied globally. In Sect. 4 we analyse the relative roles of the tropical SST and LST over Africa. Finally, in Sect. 5 we summarize the conclusions.

2 Model and experiments

The model used in this study is the Abdus Salam International Centre for Theoretical Physics (ICTP) AGCM (Molteni 2003; Kucharski et al. 2006) which is a full atmospheric model with simplified physics. We use the model version 41 in its 8-layer configuration and T30 (3.75° × 3.75°) horizontal resolution. A slab ocean model is coupled. Present-day boundary surface conditions, orbital parameters and greenhouse forcing are used. A monthly-varying ocean heat flux correction is imposed in order to keep the simulated SST close to present-day conditions. The model has been used extensively to explore climate variability over South America (e.g. Barreiro et al. 2014; Barreiro 2010; Barreiro and Tippmann 2008). In particular, in austral summer over South America and the adjacent Atlantic Ocean the model reasonably reproduces the main precipitation features (the ITCZ and the SACZ), although with a distribution more concentrated in spots compared to observations. The simulated continental (oceanic) SACZ is stronger (weaker) than in observations. The model performance regarding atmospheric circulation over South America is also satisfactory (Haarsma et al. 2005).

Three extratropical forcing patterns are implemented. The first forcing pattern consists in cooling of the SH and warming of the NH poleward of 40°, applied only over ocean grid points, and with a resulting global average forcing equal to zero. This pattern is similar to the one used in Kang et al. (2008) and TB2015 and it is intended to represent the asymmetric temperature changes associated with glacial-interglacial and millennial-scale climate variability. It may also represent the asymmetric SST pattern characteristic of the global warming trend. The forcing pattern is superposed on a background state and is obtained as explained in TB2015. The second and third forcing patterns are obtained as the NH and SH components of this forcing, respectively.

The three selected extratropical forcing patterns are shown in Fig. 1. The sign convention selected is positive out of sea. Therefore, positive values of the forcing could be thought as representing a situation where the atmosphere is dry and colder than the ocean below it so that there is a strong ocean-to-atmosphere net heat flux. Alongside with the three perturbed runs associated with each of the forcing patterns a Control run in which no forcing is applied is implemented using the same model configuration. The experiments are named *nh + sh_forcing*, *nh_forcing*, *sh_forcing* and *Control*, respectively.

A model configuration in which the tropical (30°S–30°N) SSTs are kept fixed, while the slab ocean is applied elsewhere, is implemented to test the role of these SSTs in transmitting the signal from the extratropical regions to the tropics. For this configuration we conduct three forced experiments, applying the nh + sh, nh or sh forcing patterns, as well as a corresponding Control case. The experiments names are: *nh + sh_forcing_fix_trop_sst*, *nh_forcing_fix_trop_sst*, *sh_forcing_fix_trop_sst* and *Control_fix_trop_sst*, respectively.

Finally, to asses the role of the LST over Africa, we conduct a last series of simulations in which the tropical SSTs are kept fixed, the slab ocean model is applied elsewhere and, in addition, the LST over the African continent are not allowed to change (climatological temperatures of the land model are imposed). These experiments are named: *nh + sh_forcing_fix_trop_sst_fix_Africa*, *nh_forcing_fix_trop_sst_fix_Africa*, *sh_forcing_fix_trop_sst_fix_Africa* and *Control_fix_trop_sst_fix_Africa*, respectively.

In all the simulations the model was run for 40 years and the last 10 are used for averaging. Running the simulations for 40 years proved to be more than enough to reach the equilibrium; a time scale of 10 years was estimated to be the time span necessary for adjustment. In Table 1 we summarize the experiments.

3 Response to extratropical forcing

In this section we display the results for the experiments in which the slab ocean model is applied globally. Most of the results are presented in the form of anomalies with respect to the corresponding control case. As the SACZ peaks in austral summer we will focus on this season, showing the DJF means.

3.1 SACZ

To gain insight on the magnitude of the response to the imposed forcing we will show the global anomalies for the near surface air temperature (NSAT) while for the rest of the fields we will focus on the vicinity of the SACZ displaying the anomalies only in the region 60°S–30°N, 270°E–30°E, which includes South America and tropical and southern Atlantic Ocean (SATSA).

Figure 2 shows the DJF NSAT anomalies for the *nh + sh_forcing*, *nh_forcing* and *sh_forcing* experiments. For the experiment *nh + sh_forcing* the response consists of a generalized warming (cooling) over the NH (SH) with absolute magnitudes decreasing from 70°N (70°S) toward the Equator. In the extratropics the most extreme response

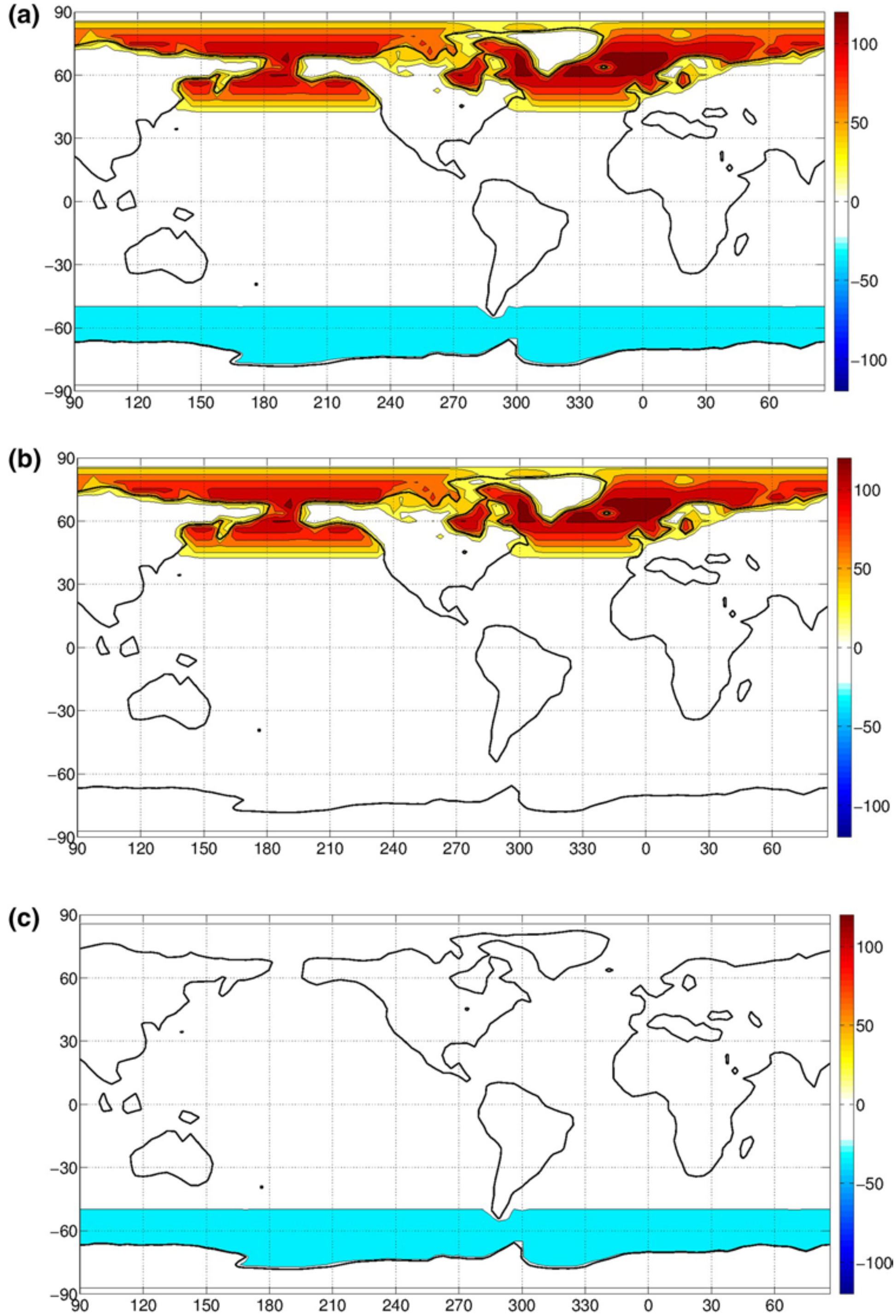

Fig. 1 Forcing pattern with components in: **a** both hemispheres, **b** NH and **c** SH. The sign convention is positive out of sea. Contour interval 20 W/m[2]

in the NH (SH) is a 16 °C (−20 °C) anomaly over the north Atlantic Ocean at 70°N (over the Ross Sea). For comparison, in a simulation of the transient evolution of climate for the last 21.000 years (TRACE2k experiment, He 2011) anomalies of about −10 °C (6 °C) are obtained over the North Atlantic (Antarctica) during HS1.

In the tropics the maximum response (11 °C) is obtained over the Sahara desert while over the oceans the signal has a W–E gradient in the northern tropics and an E–W gradient in the southern tropics, being the oceanic signal stronger in the NH than in the SH. Finally, in the SACZ region the response to the extratropical forcing is weak (below −1 °C).

In the *nh_forcing* experiment (Fig. 2b) the response in the NH high latitudes is similar to the one obtained in the *nh + sh_forcing* experiment. Although weak (less or

Table 1 Experiment summary

Experiment name	Forcing pattern	Fixed tropical SST	Fixed land surface temperature over Africa
Control	None	No	No
nh + sh_forcing	nh + sh	No	No
nh_forcing	nh	No	No
sh_forcing	sh	No	No
Control_fix_trop_sst	None	Yes	No
nh + sh_forcing_fix_trop_sst	nh + sh	Yes	No
nh_forcing_fix_trop_sst	nh	Yes	No
sh_forcing_fix_trop_sst	sh	Yes	No
Control_fix_trop_sst_fix_Africa	None	Yes	Yes
nh + sh_forcing_fix_trop_sst_fix_Africa	nh + sh	Yes	Yes
nh_forcing_fix_trop_sst_fix_Africa	nh	Yes	Yes
sh_forcing_fix_trop_sst_fix_Africa	sh	Yes	Yes

equal to 1 °C) there is some response in the SH. Over the SACZ a small region of positive NSAT anomalies is produced. For the *sh_forcing* experiment (Fig. 2c) the NSAT signal in the extratropics of the SH is similar to the one obtained in the *nh + sh_forcing* experiment and a weak (smaller than −2 °C) signal in the opposite hemisphere of the forcing is also created. Over the SACZ a temperature anomaly of −1 °C is detected. Overall, in terms of NSAT, the response to the forcing components is quasi linear being the differences between the sum of the responses of experiments with hemispheric forcing and the one with *nh + sh_forcing* experiment less than 1 °C in absolute value.

Figure 3 depicts the precipitation anomalies for the three experiments, in the SATSA sector. The strongest response is seen in the tropical band: the ITCZ is clearly shifted northward over western South America and Africa, while over eastern South America and the Atlantic ocean the ITCZ weakens. The SACZ is weakened and slightly shifted southward. Furthermore, a region of positive precipitation anomalies is generated in the Atlantic Ocean around 20°N–30°N with a SW–NE diagonal orientation. It is to be noted this region should not be regarded as a northward displacement of the ITCZ but as a secondary convergence zone itself: note the Control precipitation overlaid in Fig. 3a. We will name this new precipitation feature the North Atlantic Convergence Zone (NACZ). Also, significant positive precipitation anomalies are noted over the SALLJ region, east of the Andes.

The hemispheric simulations (Fig. 3b, c) show signals in the SATSA region, being the *nh_forcing* simulation the one that produces the strongest anomalies. The northward displacement of the ITCZ over Africa and the NACZ are reproduced by the *nh_forcing* experiment, but not by the SH counterpart.

Regarding the SACZ, the anomalies produced by the NH forcing are similar to the ones obtained when the forcings are applied in the two hemispheres. On the other hand, the application of the SH forcing produces only a weak positive anomalous signal. In this latter case the ITCZ clearly shifts northward over the western Atlantic basin. Thus, while in the ITCZ region both forcings tend to induce changes of the same sign, in the SACZ region the NH and SH forcings tend to oppose each other but with different strengths so that the NH forcing dominates the response in the experiment with combined forcing.

The similarity in the tropical surface response between the *nh + sh_forcing* and the *nh_forcing* experiments is clearly seen in the maps of mean sea level pressure (MSLP) over the whole Atlantic basin (Fig. 4). The differences arise in the response over the SH extratropics where there are quasi zonally symmetric negative (positive) anomalies southward (northward) of 50°S, which are consequence of the SH forcing (Fig. 4a, c). Also, there is an intensification of the south Atlantic subtropical high as result of both the NH and SH forcing. This response supports the fact that the SH forcing does not have a significant influence over the northern Atlantic, while the NH forcing indeed has an important influence on the South Atlantic.

The DJF near surface (950 hPa) wind changes with respect to the control in the SATSA region are shown in Fig. 5 and are thoroughly consistent with the MSLP response and shift in the precipitation bands. In the *nh + sh_forcing* and *nh_forcing* experiments the strongest changes (10 m/s) occur over western equatorial Africa in agreement with a northward displacement of the ITCZ and over the NACZ. There are also strong wind changes around 50–60°S, 270–300°E in the Southern Ocean, which are present in the *nh + sh_forcing* and s*h_forcing* experiments, which represent an intensification of the midlatitude

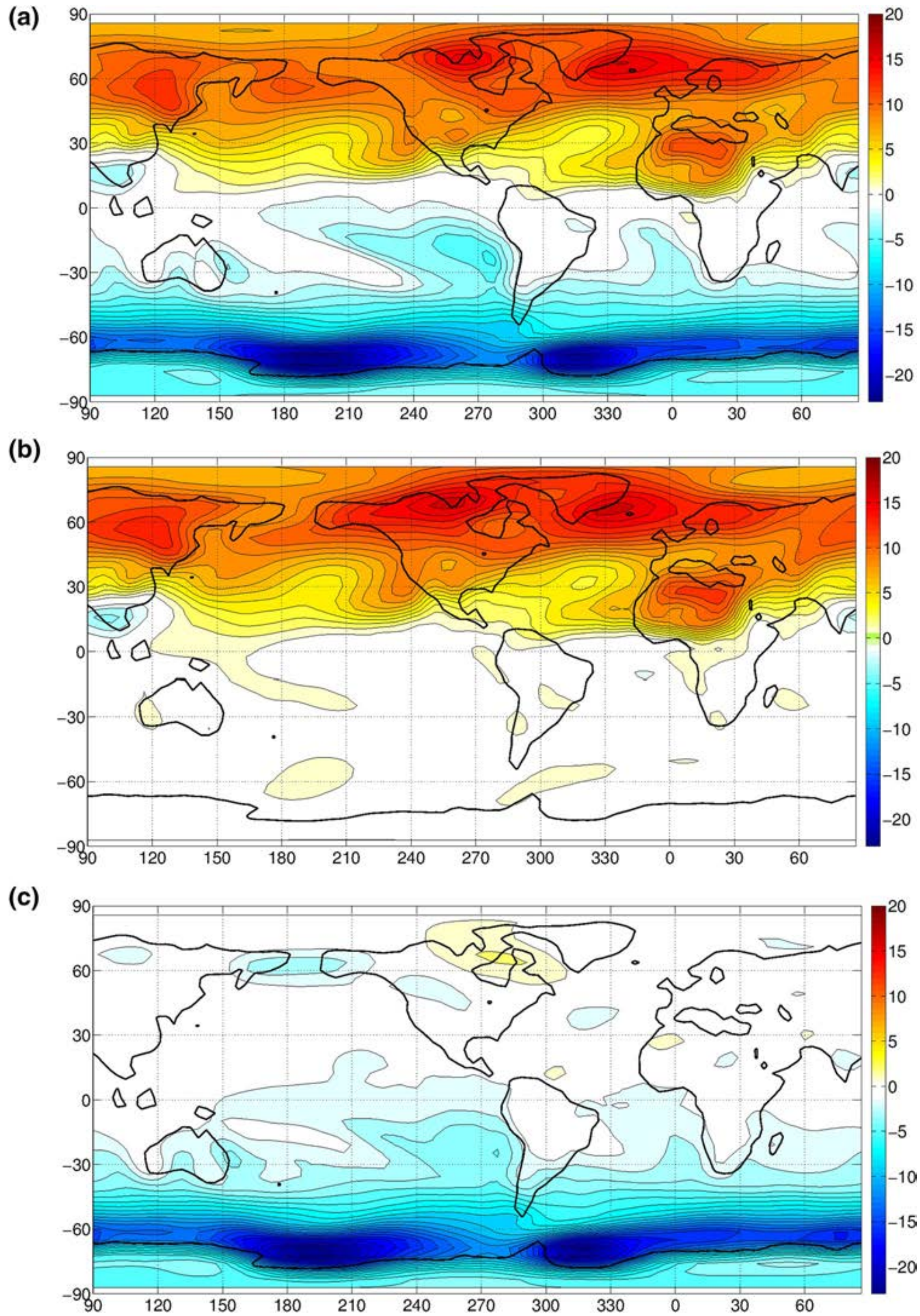

Fig. 2 DJF mean anomalies with respect to the control of NSAT for: **a** *nh* + *sh_forcing*, **b** *nh_forcing* and **c** *sh_forcing* experiments, respectively. Contour interval 1 °C

westerlies in the region. Over the SACZ a weak anticyclonic anomaly is generated and seen in the experiments involving NH forcing. An intensification of the SALLJ is also noticed when the SH component of the forcing is applied, favouring moisture convergence east of the Andes over 30ºS, consistent with an increase in the precipitation over that region.

To analyse the mean meridional circulation we consider the mass streamfunction Ψ_M defined as (e.g. Hartmann 1994): $\Psi_M = \frac{2\pi a \cos(\theta)}{g} \int_0^p [v]dp$ where a is Earth's radius, θ the latitude, g gravity, p pressure, v meridional wind and the square brackets denote zonal averages.

With an over bar denoting DJF temporal mean, Fig. 6 (panels a and b) depicts the mean meridional overturning circulation stream function $[\overline{\Psi}_M]$ anomalies with respect to the control run, calculated just over the Atlantic Ocean sector (defined as the portion of the globe between 307.5°E

Fig. 3 DJF mean anomalies with respect to the control of precipitation for: **a** *nh + sh_forcing*, **b** *nh_forcing* and **c** *sh_forcing* experiments, respectively, in the SATSA region. Contour interval 50 mm/month. For reference, in **a**, the Control precipitation is plotted in *dashed lines* with contour interval 50 mm/month

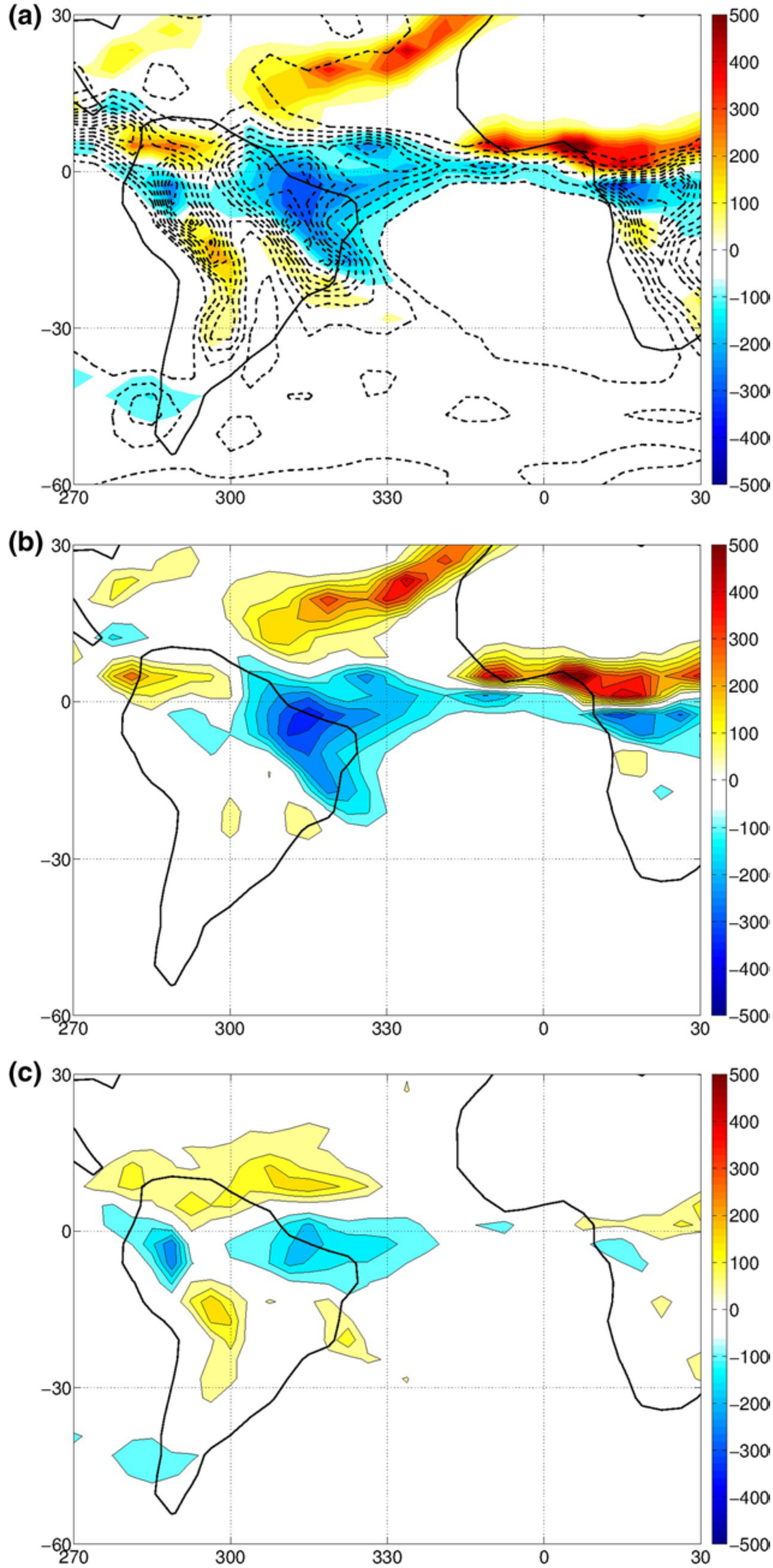

Fig. 4 DJF mean anomalies with respect to the control of MSLP for: **a** *nh + sh_forcing*, **b** *nh_forcing* and **c** *sh_forcing* experiments, respectively, in the SATSA region. Contour interval 1 hPa

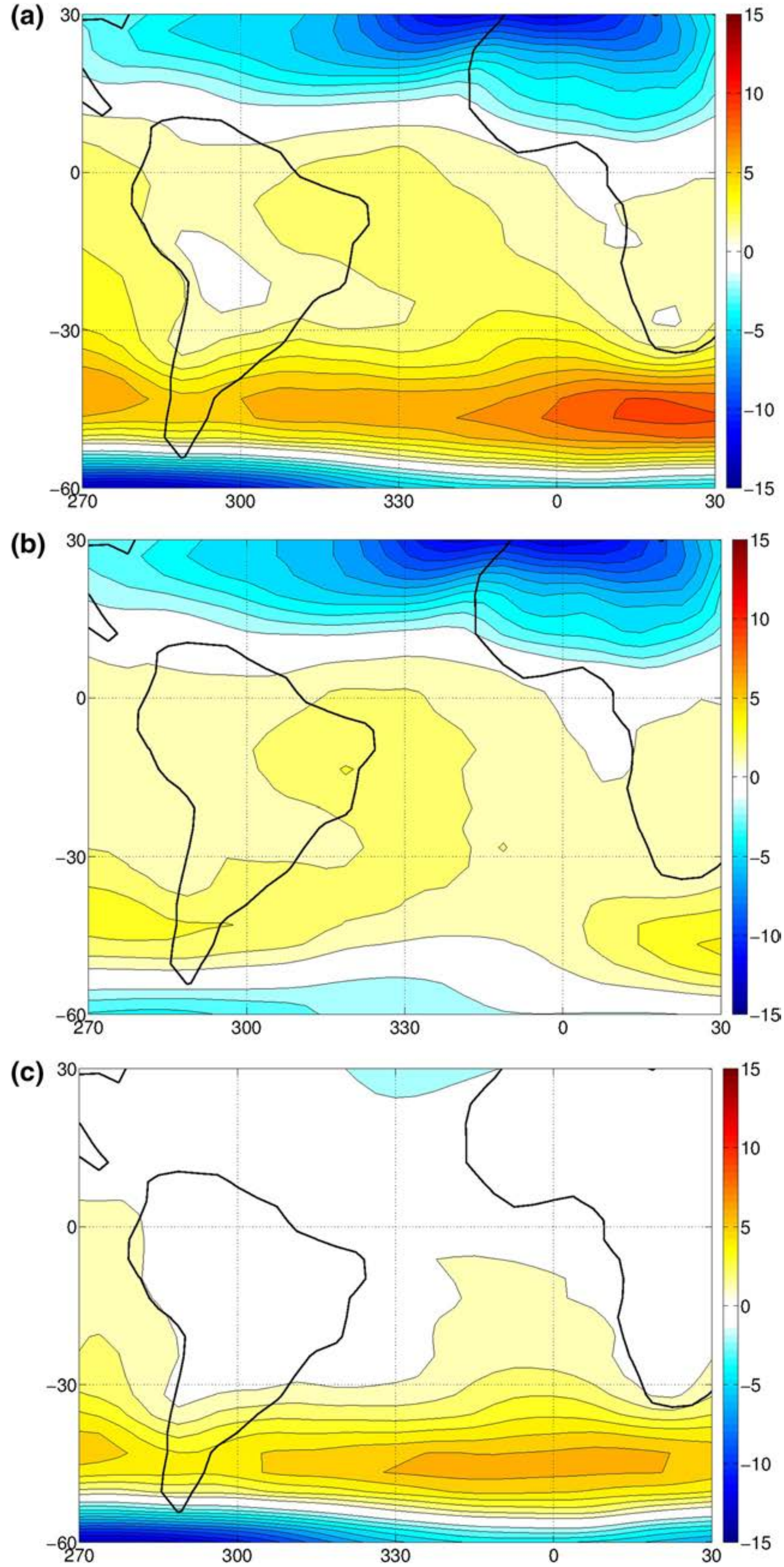

Fig. 5 DJF mean anomalies with respect to the control of near surface (950 hPa) wind for: **a** *nh + sh_forcing*, **b** *nh_forcing* and **c** *sh_forcing* experiments, respectively, in the SATSA region. Contour interval 1 m/s

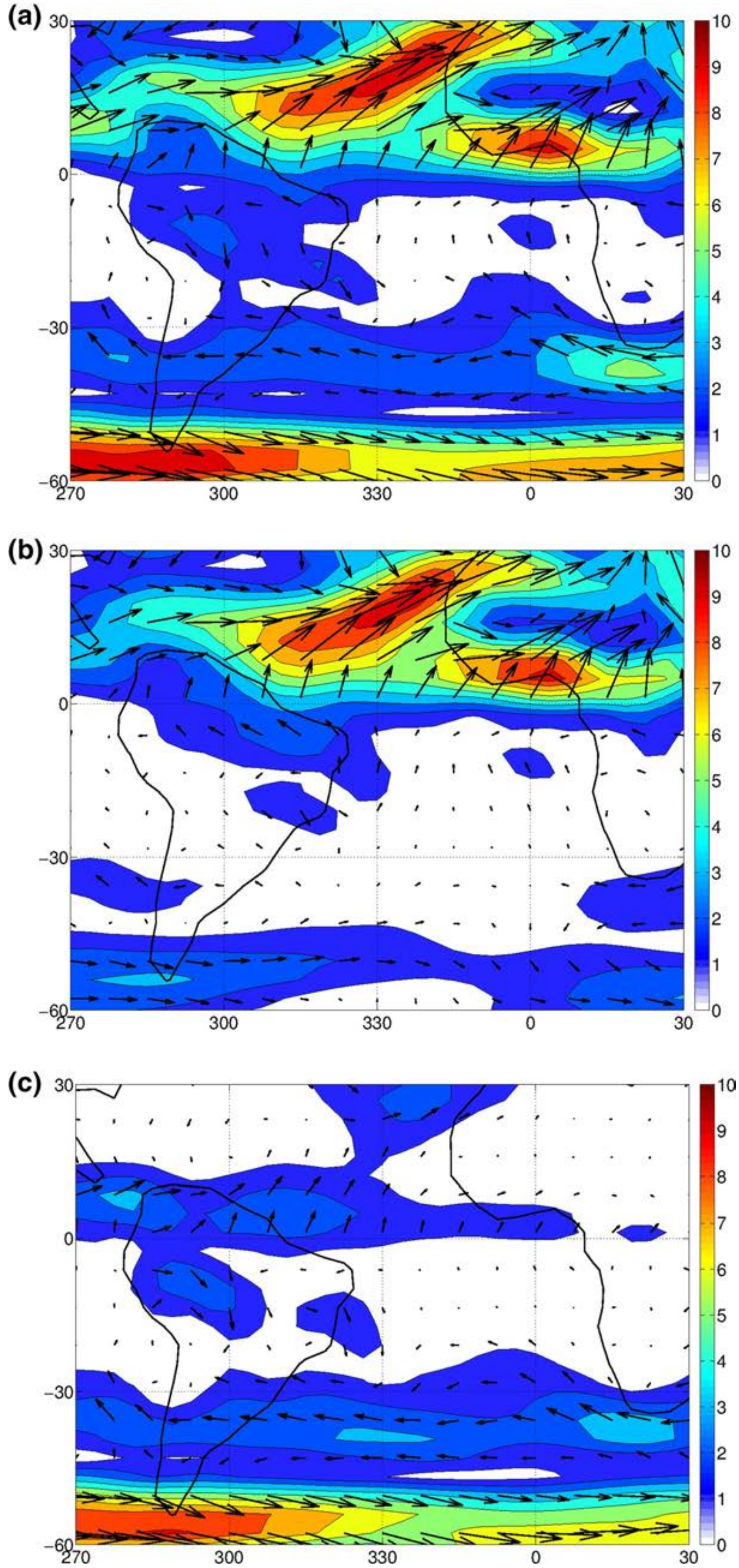

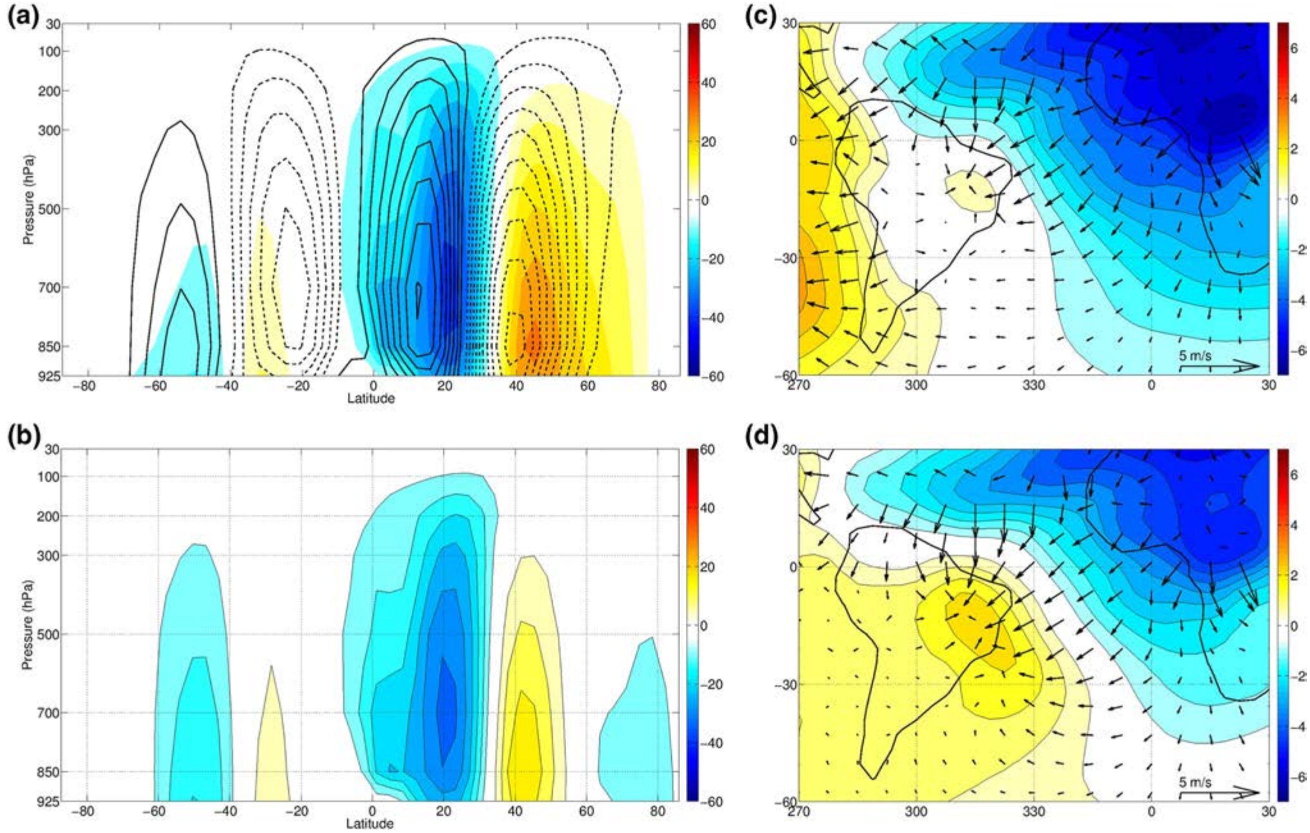

Fig. 6 **a, b** DJF mean anomalies with respect to the control of mean meridional overturning circulation stream function over the Atlantic Ocean sector /10^{10} for the *nh + sh_forcing* and *nh_forcing* experiments, respectively. Contour interval 5 m^2/s. The Control stream function is plotted in a with the same contour interval (negative values in *dashed lines*). **c, d** DJF mean anomalies with respect to the control of velocity potential (×10^6) and divergent wind for *nh + sh_forcing* and *nh_forcing*, respectively. Contour interval 0.5 m^2/s

and 7.5°E), for the *nh + sh_forcing* and *nh_forcing* experiments. The control $[\overline{\Psi}_M]$ is plotted in dashed lines over Fig. 6a to facilitate the interpretation.

The *nh + sh_forcing* produces a negative anomaly region from 10°S to 30°N, indicating that a new uplift region is created around 30°N in the Atlantic, in agreement with the convergence of surface winds and development of the NACZ (Fig. 6a). As result there is a weakening of the northern Hadley cell and an intensification of the southern cell, associated with increased descent over the SACZ. In addition, a region of strong positive anomalies is found from 30°N to 70°N indicating changes in the Ferrel Cell.

The hemispheric experiments indicate that the SH forcing produces a weak response in terms of stream function (not shown). On the contrary, the NH forcing creates a similar anomaly pattern to the one created in the *nh + sh_forcing* experiment, in agreement with the similarities in the surface fields described previously (Fig. 6b).

Overall, we can conclude that the total response to the extratropical thermal forcing is predominantly linear with respect to the NH and SH components of the forcing. In particular, the SACZ is weakened by the forcing and this weakening is still produced when only the NH component of the forcing is applied. When the SH component is the only forcing, the SACZ shows some strengthening, which is overcome by the NH forcing. Thus, results indicate that the NH forcing exerts the strongest control on the SACZ's behaviour.

To complement the picture, the velocity potential and divergent wind anomalies at 200 hPa for the *nh + sh_forcing* and *nh_forcing* experiments are shown in Fig. 6c, d. For the experiment *nh + sh_forcing* a region of upper-level divergence (convergence) is noticed over the north tropical Atlantic (SACZ). Over the SACZ, the strongest gradient of the velocity potential (strongest convergent wind) is noted in two directions: a N–S component originating from the NACZ, and a NE–SW component originating from western equatorial Africa.

The hemispheric experiments indicate that the NH component of the forcing is the one that produces the upper-level convergence over SACZ, being the generated anomalies even stronger than those seen in the *nh + sh_forcing* simulation. The SH component of the forcing produces a weak signal over the SACZ, in the opposite direction (generating a weak divergence over the region; not shown), consistent with changes in precipitation mentioned above.

In view of these results we hypothesize that the NACZ plays a main role in the signal transmission from the NH extratropics to the SACZ, arguing that the anomalous uplift region associated with the NACZ promotes changes in the Hadley circulation over the tropical Atlantic Ocean in which anomalous descent is favoured over the SACZ, thus inhibiting the development of precipitation (see Fig. 6c, d) and generating the SACZ weakening. To test this hypothesis we will proceed in two steps. First, we will analyse how the NACZ is generated considering both upper-level and surface controlling factors. Second, we will design a new experiment in which the NACZ is inhibited to develop in response to the extratropical forcing.

3.2 NACZ

In this subsection we analyse the surface and upper-level factors that favour the generation of the NACZ, as we consider that its development is fundamental to understand the response of the SACZ to the extratropical forcing. As mentioned before, the NACZ is a precipitation feature generated when the NH extratropical forcing is applied. Therefore, for briefness, we will only focus in the experiment in which the extratropical forcing has components in the two hemispheres.

Figures 2, 3, 4 and 5 showed that, in the presence of the NH extratropical component of the forcing, the surface conditions are favourable for the development of the NACZ: when the extratropical forcing in the NH is imposed it strongly weakens the north Atlantic subtropical high (Fig. 4), weakening the trades (Fig. 5) and generating a positive SST anomaly to the north of the Equator (see Fig. 2 for NSAT). This induces anomalous surface wind convergence between 20°N and 30°N, prompting the development of the NACZ.

At the same time, changes in the upper-level configuration might also be favorable for the NACZ. Figure 7 shows the total (not anomaly, to simplify the analysis) precipitation and streamfunction at 200 hPa for the experiments *Control* and *nh + sh_forcing* in the SATSA region. For the Control case, it can be seen that the model successfully reproduces the observed relationship between the SACZ and the upper-level circulation (see Garreaud and Aceituno 2007 for an observational analysis): the SACZ is located between an anticyclonic circulation over Bolivia and a cyclonic circulation over northeastern Brazil. Meanwhile, the 200 hPa configuration in the northern tropics is quasi-zonal, being the ITCZ the only significant precipitation feature produced. For the *nh + sh_forcing* experiment, as the heat source is displaced northward (due to the northward displacement of the ITCZ in Fig. 3a) two anticyclones with downstream troughs are now evident at both sides of the Equator consistent with a Gill-type response to a symmetric equatorial heating (Gill 1980). The downstream upper-level troughs favour the development of surface convergence zones in both hemispheres (SACZ and NACZ). Note that the SACZ becomes weaker than in the *Control* experiment in agreement with a weaker 200 hPa cyclonic circulation.

In summary, both surface and upper-level conditions are favorable for the development of the NACZ when the NH component of the extratropical forcing is applied. On one hand, there is a local and direct SST effect: warming of the surface waters on the northern flank of the Equator in the tropical Atlantic induces local convergence of winds. On the other hand, there is an indirect effect derived from the shifting of the heat source (due to tropical SST anomalies): the NH part of the extratropical forcing displaces the heat source northwards, generating a Gill-type response symmetric about the Equator, generating favorable conditions for the development of convergence zones at both sides of the Equator.

Given this analysis, we argue that to discourage the development of the NACZ it is necessary to inhibit both the direct SST effect and the indirect response due to the heat source displacement. As the heat source displacement over SATSA is mainly produced by the effect of the extratropical forcing on the tropical SST (TB2015), we propose that by not allowing the tropical SST to react to the extratropical stimulus, the NACZ will not find the conditions to develop. Then, to test our proposed mechanism of transmission of information from the NH extratropics to the SACZ via the NACZ, we perform additional experiments in which the tropical SST is not allowed to respond to changes in the surface heat fluxes.

4 Roles of tropical SST and LST over Africa

We start this section briefly presenting the results in which the extratropical forcing (with its components in the two hemispheres) is applied, but the tropical SSTs are not allowed to change.

Figure 8a shows the DJF precipitation anomalies for the experiment *nh + sh_forcing_fix_trop_sst* with respect to the corresponding control case for this configuration, for the SATSA area. As expected based on above discussion, the NACZ completely vanishes. The response over the ITCZ is greatly reduced although some significant signal is still present over the Atlantic Ocean and Africa. Over the SACZ there is still some response indicating a weakening and slight southward shift as in the *nh + sh_forcing* but changes are much weaker (75% reduction in the signal calculated in the box defined as: 17°S–9°S, 315°E–330°E). The signal obtained in the *nh + sh_forcing_fix_trop_sst* experiment is

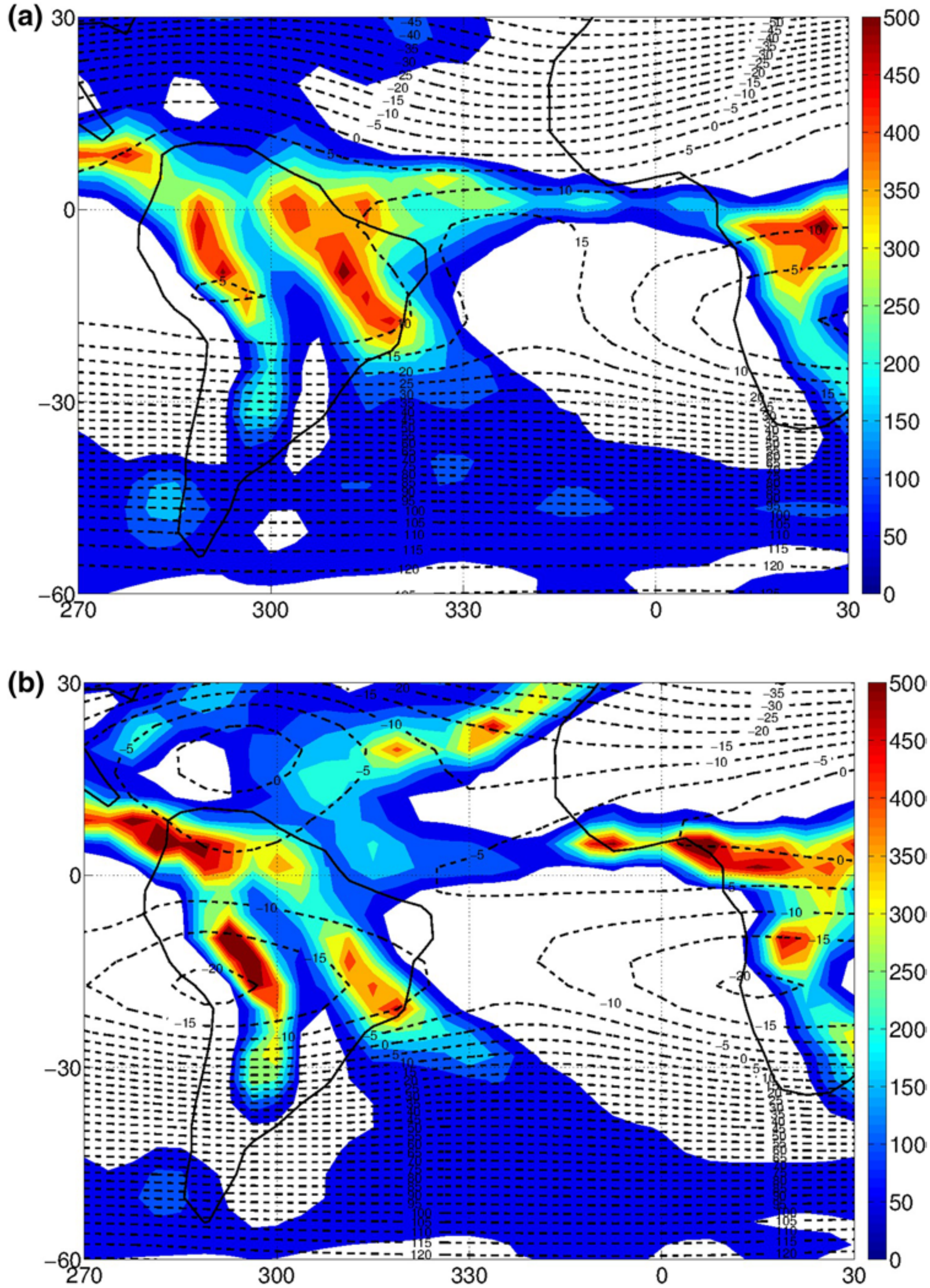

Fig. 7 DJF Total precipitation (shaded) and 200 hPa horizontal stream function /10^6 (*dashed lines*) for: **a** Control and **b** *nh* + *sh_forcing* experiments, respectively. Contour interval for precipitation: 50 mm/month. Contour interval for stream function: 5 m^2/s

mostly reproduced by applying the NH portion of the forcing, in particular the northward displacement of the ITCZ over Africa and the weakening over SACZ; the SH forcing produces some signal over SACZ but is weak and of minor extension (not shown).

In the absence of tropical SST response the surface wind response is weaker in all the SATSA region, except in the midlatitudes where an intensification of the westerlies is still triggered and over the SALLJ where an intensification also takes place (not shown). The 200 hPa divergent wind anomalies over the SACZ are weaker (Fig. 8b) although a component originating in the region of ITCZ northward displacement over western equatorial Africa can be appreciated.

Therefore, the results obtained in this section confirm that in the absence of the NACZ, the SACZ response is much weaker remaining about 25% of the signal. Is it possible to explain the other 25% by changes in the ITCZ in western Africa? TB2015 found that the ITCZ response over Africa completely vanishes when, in addition to fixed tropical SST, the LST over Africa is not allowed to change. Therefore, to test the hypothesis that the remaining

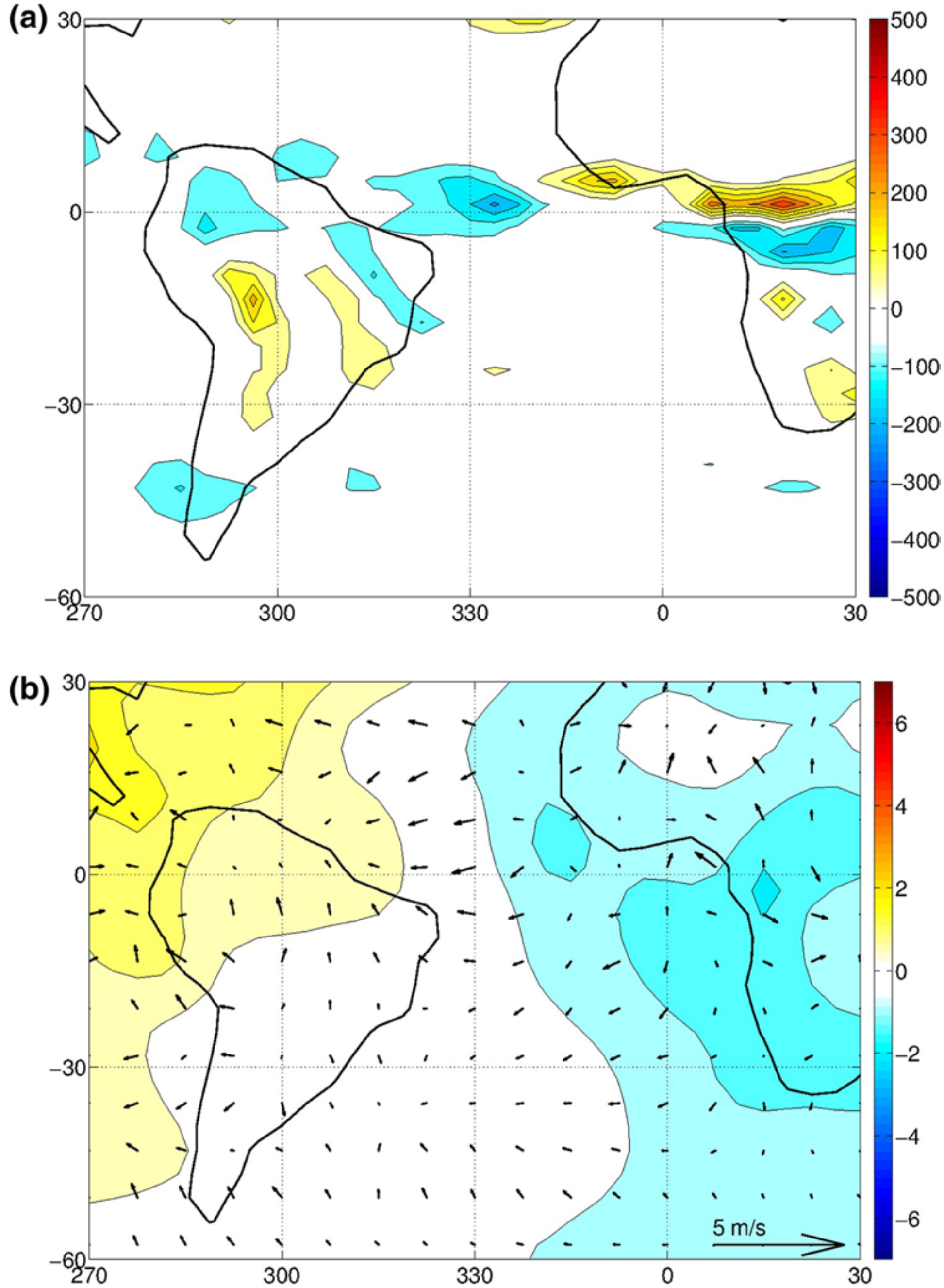

Fig. 8 *nh + sh_forcing_fix_trop_sst* DJF mean anomalies with respect to the control in the SATSA region of: **a** precipitation (contour interval 50 mm/month) and **b** velocity potential ($\times 10^6$) and divergent wind (contour interval 0.5 m^2/s)

25% of the SACZ' signal is remotely induced by the ITCZ changes over Africa, we conduct a last series of simulations in which both tropical SSTs and LSTs over Africa are kept fixed. In Fig. 9 we show the results for the simulation with forcing in the two hemispheres.

As expected, the precipitation anomalies over Africa completely vanish while over the SACZ, although there are still some anomalies present, are reduced considerably (Fig. 9a). Divergent wind in upper levels (Fig. 9b) agree with the results of precipitation, not showing any significant signal over the SACZ.

5 Summary and conclusions

We investigated the response of the SACZ to an extratropical thermal forcing in an AGCM coupled to a slab ocean model, with realistic surface boundary conditions. The imposed forcing consists of warming of the NH and cooling of the SH, with zero global mean. We further divide the forcing into its northern and southern components to assess their relative roles in affecting the SACZ.

We found that during its peak season (DJF) the SACZ is affected by the imposed extratropical forcing and,

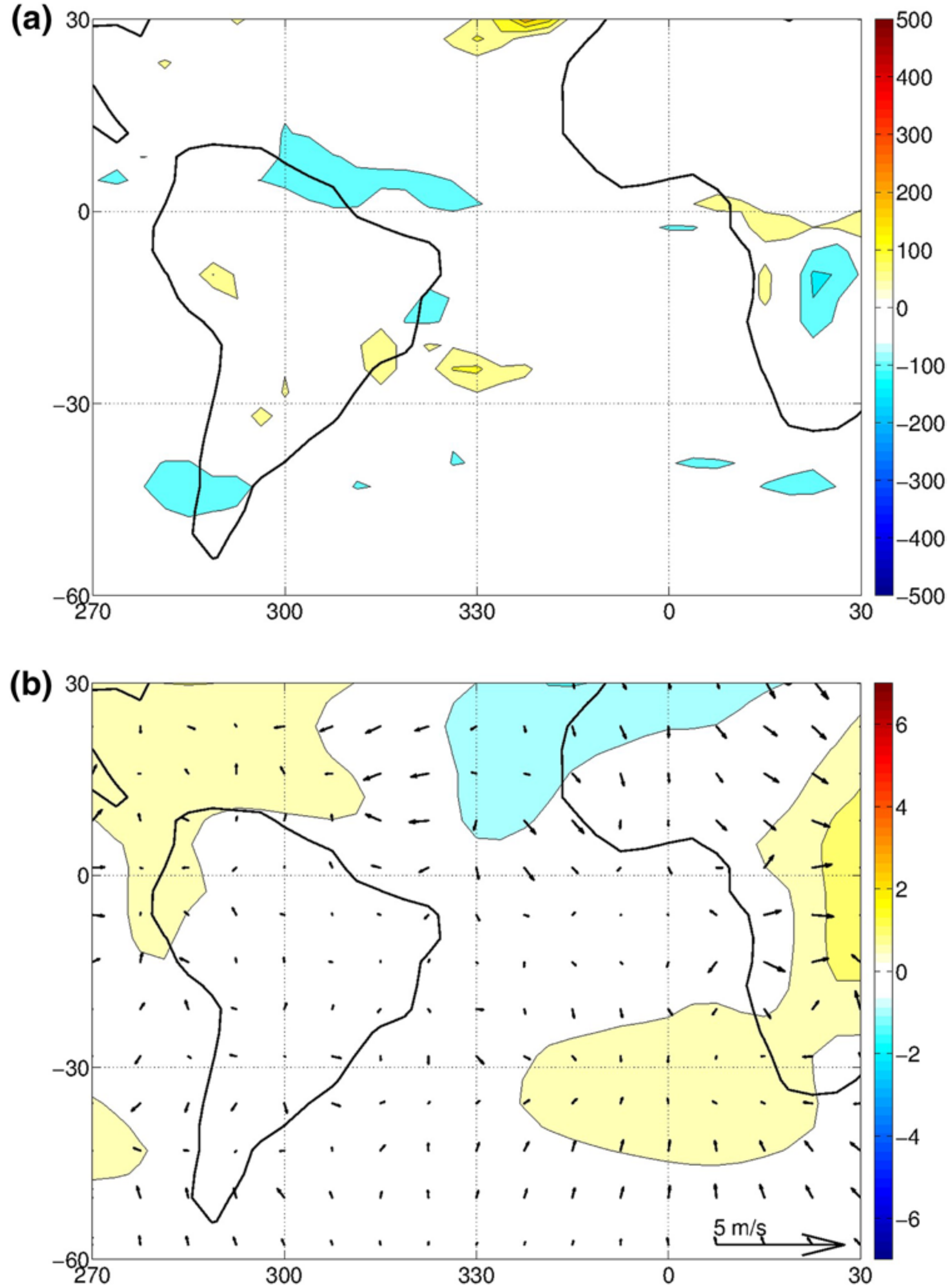

Fig. 9 Same as Fig. 8 for the experiment *nh + sh_forcing_fix_trop_sst_fix_Africa*

fundamentally, by the NH. The SACZ response to a warming of the NH and cooling of the SH extratropics consists of a weakening, a different behaviour from the one displayed by the ITCZ which tends to respond to the same forcing by shifting towards the anomalously warmer Hemisphere.

These results are in agreement with the paleoclimatic and modeling studies that analyse the SACZ response to extratropical forcings.

From Stríkis et al. (2015), and assuming linearity of the processes, a warming of the NH would lead to a SACZ weakening and a northward ITCZ shift over South America. Our results agree and also indicate that in the event of a NH warming the SACZ is weakened and that a northward ITCZ displacement occurs over western South America. However, in our simulations the eastern South America's ITCZ does not shift but weakens, a discrepancy that could be model dependent.

Chiessi et al. (2009) proposed two mechanisms linking the SACZ to the AMO. The first mechanism implied that a cooling of the western South Atlantic would lead to a SACZ weakening. This local effect of the Atlantic SST on the development of the SACZ has been studied in observations as well as in model simulations (Jorgetti et al. 2014; Barreiro et al. 2002). However, we can not make any statements on this regard given that in our simulations such mechanism was not triggered (no significant SST changes were found in the vicinity of the SACZ in the western south Atlantic). The second mechanism associated a northward South American ITCZ shift with a SACZ weakening, which is in agreement with our results although we did not find any evidence related to changes in the low level jet (see Fig. 5b) as was suggested by Chiessi et al. (2009).

Regarding other model simulations, our findings are in agreement with the ones of Junquas et al. (2012) which indicate that the case of a NH warmer than the SH is expected to produce a weakening of the SACZ during DJF.

We further proposed that the communication of the signal from the northern extratropics to the SACZ is produced by two overlapping mechanisms. The first mechanism is related to the generation of a secondary convergence zone in the northern tropical Atlantic (NACZ): when the forcing is applied, changes in the general circulation of the atmosphere are such that a region of surface wind convergence is generated over the Atlantic Ocean in the latitude band 20°N–30°N; this convergence and its associated ascent region induce changes in the Hadley circulation that promotes anomalous descent over the SACZ, inducing a precipitation decrease there. The second mechanism, explaining the remaining 25% of the precipitation decrease, relates changes in the African ITCZ to the SACZ: the extratropical forcing induces a northward ITCZ displacement over Africa, which via an anomalous zonal circulation favours subsidence over the northern portion of the SACZ and a consequent decrease in precipitation.

To test the viability of the proposed mechanisms we designed new experiments in which the same forcing patterns are applied but the model configuration is modified.

To test the first mechanism we conducted simulations in which the NACZ is not developed: simulations with fixed tropical SST. In this case the SACZ precipitation anomalies weaken significantly (75% of signal reduction) highlighting the fundamental role of the tropical SSTs in transmitting the information from the high latitudes to this tropical convergence zone.

The remaining 25% of the precipitation signal over the SACZ was linked to the second proposed mechanism via simulations in which, in addition to fixed tropical SSTs, a restriction over the LST over Africa was imposed. As shown in TB2015, not allowing the tropical SSTs nor the LST over Africa to change in response to the remote extratropical forcing will lead to the vanishing of the African ITCZ response and, in this case, this was also associated to the weakening of the SACZ precipitation signal.

In summary, we found that the SACZ response to a warming of the NH and a cooling of the SH high latitudes consists in a precipitation decrease, and that the NH component of the forcing is the one that plays the dominant role. It would be desirable to repeat the experiments with other models and to search for this type of signal in climate change projections and Last Glacial Maximum simulations.

Acknowledgements Part of this work was performed while the first author was supported by grants from Universidad de la República and Agencia Nacional de Investigación e Innovación (ANII), Uruguay.

References

Barreiro M (2010) Influence of ENSO and the South Atlantic Ocean on climate predictability over Southeastern South America. Clim Dynam 35:1493–1508. doi:10.1007/s00382-009-0666-9

Barreiro M, Tippmann A (2008) Atlantic modulation of El Nino influence on summertime rainfall over southeastern South America. Geoph Rese Lett. doi:10.1029/2008GL035019

Barreiro M, Chang P, Saravanan R (2002) Variability of the South Atlantic convergence zone simulated by an atmospheric general circulation model. J Clim 15:745–763

Barreiro M, Díaz N, Renom M (2014) Role of the global oceans and land–atmosphere interaction on summertime interdecadal variability over northern Argentina. Clim Dynam 42:1733–1753. doi:10.1007/s00382-014-2088-6

Carvalho LM, Jones C, Liebmann B (2004) The South Atlantic convergence zone: intensity, form, persistence, and relationships with intraseasonal to interannual activity and extreme rainfall. J Climate 17:88–108. doi:10.1175/1520-0442(2004)017<0088:TSACZI>2.0.CO;2

Chiang JC, Bitz CM (2005) Influence of high latitude ice cover on the marine Intertropical Convergence Zone. Clim Dynam 25:477–496. doi:10.1007/s00382-005-0040-5

Chiessi, CM, Mulitza S, Pätzold J, Wefer G, Marengo JA (2009). Possible impact of the Atlantic Multidecadal Oscillation on the South American summer monsoon. Geophys Res Lett. doi:10.1029/2009GL039914

Cvijanovic I, Chiang JC (2013) Global energy budget changes to high latitude North Atlantic ooling and the tropical ITCZ response. Clim Dynam 40:1435–1452. doi:10.1007/s00382-012-1482-1

Doyle ME, Barros VR (2002) Midsummer low-level circulation and precipitation in subtropical South America and related sea surface temperature anomalies in the South Atlantic. J Climate 15:3394–3410. doi:10.1175/1520-0442(2002)015<3394:MLLCAP>2.0.CO;2

Figueroa SN, Satyamurty P, Da Silva Dias PL (1995) Simulations of the summer circulation over the South American region with an eta coordinate model. J Atmos Sci 52:1573–1584

Folland CK, Palmer TN, Parker DE (1986) Sahel rainfall and worldwide sea temperatures, 1901–85. Nature 320:602–607. doi:10.1038/320602a0

Friedman AR, Hwang YT, Chiang JC, Frierson DM (2013) Interhemispheric temperature asymmetry over the twentieth century and in future projections. J Climate 26:5419–5433. doi:10.1175/JCLI-D-12-00525.1

Frierson DM, Hwang YT (2012) Extratropical influence on ITCZ shifts in slab ocean simulations of global warming. J Climate 25:720–733. doi:10.1175/JCLI-D-11-00116.1

Garreaud RD, Aceituno P (2007) Atmospheric circulation over South America: mean features and variability. The physical geography of South America. Oxford University Press, Oxford

Gill A (1980) Some simple solutions for heat-induced tropical circulation. Q J Roy Meteor Soc 106:447–462

Grimm AM, Silva Dias PL (1995) Analysis of tropical-extratropical interactions with influence functions of a barotropic model. J Atmos Sci 52:3538–3555

Grimm AM, Pal J S, Giorgi F (2007) Connection between spring conditions and peak summer monsoon rainfall in South America: Role of soil moisture, surface temperature, and topography in eastern Brazil. J Climate 20:5929–5945. doi:10.1175/2007JCLI1684.1

Hartmann DL (1994) Global Physical Climatology. International Geophysics Series, vol 56, Academic Press, New York

Haarsma RJ, Campos EJ, Hazeleger W, Severijns C, Piola AR, Molteni F (2005) Dominant modes of variability in the South Atlantic: a study with a hierarchy of ocean–atmosphere models. J Climate 18:1719–1735

He F (2011) Simulating Transient Climate Evolution of the Last Deglaciation with CCSM3. Ph.D thesis, University of Wisconsin-Madison

Jorgetti T, da Silva Dias PL, de Freitas ED (2014). The relationship between South Atlantic SST and SACZ intensity and positioning. Clim Dynam 42:3077–3086. doi:10.1007/s00382-013-1998-z

Junquas C, Vera C, Li L, Le Treut H (2012) Summer precipitation variability over Southeastern South America in a global warming scenario. Clim Dynam 38:1867–1883. doi:10.1007/s00382-011-1141-y

Kang SM, Held IM, Frierson DM, Zhao M (2008) The Response of the ITCZ to Extratropical Thermal Forcing: Idealized Slab-Ocean Experiments with a GCM. J Climate 21:3521–3532. doi:10.1175/2007JCLI2146.1

Kang SM, Frierson DM, Held IM (2009) The Tropical Response to Extratropical Thermal Forcing in an Idealized GCM: The Importance of Radiative Feedbacks and Convective Parameterization. J Atmos Sci 66:2812–2827. doi:10.1175/2009JAS2924.1

Kodama Y-M (1992) Large-scale common features of subtropical precipitation zones (the Baiu Frontal Zone, the SPCZ, and the SACZ). Part I: characteristics of subtropical frontal zones. J Meteorol Soc Jpn 70:813–835

Kodama YM (1993) Large-scale common features of sub-tropical convergence zones (the Baiu Frontal Zone, the SPCZ, and the SACZ) Part II: conditions of the circulations for generating the STCZs. J Meteorol Soc Jpn 715:581–610

Kucharski F, Molteni F, Bracco A (2006) Decadal interactions between the western tropical Pacific and the North Atlantic Oscillation. Clim Dynam 26: 79–91. doi:10.1007/s00382-005-0085-5

Molteni F (2003) Atmospheric simulations using a GCM with simplified physical parametrizations. I. Model climatology and variability in multi-decadal experiments. Clim Dynam 20:175–191

Stríkis N et al (2015) Timing and structure of Mega-SACZ events during Heinrich Stadial 1. Geophys Res Lett 42:5477–5484. doi:10.1002/2015GL064048

Talento S, Barreiro M (2012) Estimation of Natural Variability and Detection of Anthropogenic Signal in Summertime Precipitation over South America. Advances Meteor. doi:10.1155/2012/725343

Talento S, Barreiro M (2015) Simulated sensitivity of the tropical climate to extratropical thermal forcing: tropical SSTs and African land surface. Clim Dynam. doi:10.1007/s00382-015-28909

Vera CS et al. (2006) Toward a unified view of the American monsoon systems. J Climate 19:4977–5000

Wang X, Auler A, Edwards RL, Cheng H, Cristalli PS, Smart PL, Richards DA, Shen C (2004) Wet periods in northeastern Brazil over the past 210kyr linked to distant climate anomalies. Nature 432:740–743. doi:10.1038/nature03067